Journal for ImmunoTherapy of Cancer

Anticoagulation therapy promotes the tumor immune-microenvironment and potentiates the efficacy of immunotherapy by alleviating hypoxia

Jeong Uk Choi,[1,2] Na Kyeong Lee,[2] Hyungseok Seo,[3] Seung Woo Chung,[4] Taslim A Al-Hilal,[5] Seong Jin Park,[2] Seho Kweon,[6] Nuri Min,[6] Sang Kyoon Kim,[7] Seohyun Ahn,[8] Uk-Il Kim,[8] Jin Woo Park,[9] Chang-Yuil Kang,[2] In-San Kim ,[10] Sang Yoon Kim,[11,12] Kyungjin Kim,[8] Youngro Byun [2,6]

To cite: Choi JU, Lee NK, Seo H, *et al*. Anticoagulation therapy promotes the tumor immune-microenvironment and potentiates the efficacy of immunotherapy by alleviating hypoxia. *Journal for ImmunoTherapy of Cancer* 2021;**9**:e002332. doi:10.1136/jitc-2021-002332

► Additional online supplemental material is published online only. To view, please visit the journal online (http://dx.doi.org/10.1136/jitc-2021-002332).

JUC and NKL are joint first authors.

Accepted 13 July 2021

For numbered affiliations see end of article.

Correspondence to
Professor Youngro Byun;
yrbyun@snu.ac.kr

ABSTRACT

Purpose Here, this study verifies that cancer-associated thrombosis (CAT) accelerates hypoxia, which is detrimental to the tumor immune microenvironment by limiting tumor perfusion. Therefore, we designed an oral anticoagulant therapy to improve the immunosuppressive tumor microenvironment and potentiate the efficacy of immunotherapy by alleviating tumor hypoxia.

Experimental design A novel oral anticoagulant (STP3725) was developed to consistently prevent CAT formation. Tumor perfusion and hypoxia were analyzed with or without treating STP3725 in wild-type and P selectin knockout mice. Immunosuppressive cytokines and cells were analyzed to evaluate the alteration of the tumor microenvironment. Effector lymphocyte infiltration in tumor tissue was assessed by congenic CD45.1 mouse lymphocyte transfer model with or without anticoagulant therapy. Finally, various tumor models including *K-Ras* mutant spontaneous cancer model were employed to validate the role of the anticoagulation therapy in enhancing the efficacy of immunotherapy.

Results CAT was demonstrated to be one of the perfusion barriers, which fosters immunosuppressive microenvironment by accelerating tumor hypoxia. Consistent treatment of oral anticoagulation therapy was proved to promote tumor immunity by alleviating hypoxia. Furthermore, this resulted in decrease of both hypoxia-related immunosuppressive cytokines and myeloid-derived suppressor cells while improving the spatial distribution of effector lymphocytes and their activity. The anticancer efficacy of αPD-1 antibody was potentiated by co-treatment with STP3725, also confirmed in various tumor models including the *K-Ras* mutant mouse model, which is highly thrombotic.

Conclusions Collectively, these findings establish a rationale for a new and translational combination strategy of oral anticoagulation therapy with immunotherapy, especially for treating highly thrombotic cancers. The combination therapy of anticoagulants with immunotherapies can lead to substantial improvements of current approaches in the clinic.

INTRODUCTION

Limited tumor perfusion leads to impaired drug delivery, deprived oxygenation and exerts detrimental effects on the tumor microenvironment (TME), which consequently decreases the efficacy of chemotherapy, immunotherapy, radiotherapy, nanomedicine and more.[1 2] Impaired tumor perfusion is attributed to the abnormal characteristics of tumor vasculature, such as high permeability, tortuosity, and compression.[3] Antiangiogenic strategies resolve this issue, in part, however, vessel normalization seems transient and the therapeutic window of drugs are restrictively narrow for effective clinical use[1 4]; thus, alternative therapeutic approaches to enhance persistent tumor perfusion seem highly relevant.[1 2 5]

The most difficult-to-overcome consequence of limited perfusion is tumor hypoxia. Hypoxia in the TME exerts immunomodulatory effects through complex interplay of cancer cells, immune cells and secretory cytokines.[6 7] There have been controversial reports of hypoxia and hypoxia-inducing factor-1α (HIF-1α)-related pathways exerting pro-inflammatory or immunosuppressive effects. Some studies insisted that hypoxia driven HIF-1α exert pro-inflammatory effects and facilitate tumor infiltration of $CD8^+$ T cells as well as enhance their function.[8–10] However, majority of these studies have limitations as they used direct elimination of only HIF-1α and artifact-prone VHL KO mice models, which are not pertinent to fully reflect the tumor infiltrating lymphocytes (TILs) exposed to the TME. Meanwhile, since Sitkovsky *et al*[11] first reported that tumor hypoxia is detrimental to adaptive immunity, series of studies in the last

two decades have widely proven that tumor hypoxia and hypoxia-related proteins and cytokines predominantly contribute to immunosuppression.[6 12] Furthermore, there are numerous reported anti-immunosuppressive benefits of hypoxia relief that, in turn, lead to enhanced effector T cell activity, improved anti-tumor immunity and tumor regression.[13] Thus, there is a growing interest in improving tumor oxygenation by strategies such as respiratory hyperoxia, oxygenation agents or HIF inhibitors to diminish immunosuppression.[13 14] Studies by groups such as Hatfield *et al*[15–18] first proved the effectiveness of elimination of hypoxia for enhancement of immunotherapy. They also found that hypoxia exerts immunosuppressive effects through hypoxia-HIF-1α-CD39/CD73-A2 adenosine receptors-cAMP-PKA-CREB-CRE, HIF-1α-HRE-mediated immunosuppressive transcription and HIF-1α-CD39/CD73-A2 adenosine receptors-cAMP-PKA mediated inhibition of TCR (T cell receptor) triggered activation of T cells.[11 13 19–21] Hence, relief of tumor hypoxia could be an attractive strategy in enhancing antitumor immunity and the efficacy of immunotherapeutic agents.

Cancer-associated thrombosis (CAT) has been well reported to be common in most solid tumors such as the cancers of pancreas, stomach, kidney, prostate and etc.[22] According to clinical statistics, the risk of developing venous thromboembolism (VTE) for patients with cancer is four times higher than for non-cancer patients.[23] This risk increases even more with chemotherapy treatment that damages blood vessels.[24]

The impact of CAT on blood perfusion and hypoxia in tumor tissue, however, has been immensely underestimated.[25] By examining human glioblastoma samples, Brat and Van Meir[26] identified that vaso-occlusion caused by intravascular thrombosis substantially affects tumor hypoxia and necrosis. Others have demonstrated, using several preclinical models, that the deposition of coagulation factors in tumor stroma can exert massive solid stress, which decompresses vessels and limits perfusion.[27] They reported that the treatment of fibrinolytic enzymes such as tissue plasminogen activator could successfully degrade the fibrin clots and thus enhance both tumor perfusion and drug delivery. While evidence indicates that the formation of CAT in tumor vessels and stroma are positively correlated with the decreased perfusion and accelerated hypoxia, systematic observations or underlying mechanisms have yet to be elucidated.[28] In this regard, we hypothesized that blood clots formed in blood vessels and interstitial areas of the tumor act as a major transport barrier that reduces tumor perfusion and aggravate hypoxia. Therefore, we also speculated that the constant use of proper anticoagulants could alleviate hypoxia, altering the TME to become more immune-supportive, which would also augment the efficacy of immunotherapy.

Low-molecular-weight heparin (LMWH) has extensively been used in the clinic as the treatment option for CAT in cancer patients, as it has many advantages in its reliability in efficacy and safeness.[29] However, as it is not orally available, direct oral anticoagulants (DOACs) are used increasingly as a consensus guideline for treating CAT in replacement of LMWH.[30 31] In order to overcome this limitation and to further improve its pharmacokinetics, we have previously developed an orally active heparin conjugate, namely STP3725 as a new DOAC, which is a conjugate of enoxaparin and tetrameric deoxycholates.[32] We have found that STP3725 is orally active with 26.3% of oral bioavailability in rats and that its administration successfully prevented the formation of VTE in animal models. In this study, we validated our hypothesis that CAT is a major barrier, which can limit tumor perfusion and aggravate tumor hypoxia. We also verified that the administration of STP3725 potentiates the efficacy of immunotherapy by reducing hypoxia and fostering an immune-supportive microenvironment.

METHODS

STP3725 synthesis and formulation

STP3725 was previously developed by site-specific conjugation of a tetradeoxycholic acid to the end-site of enoxaparin.[32] The synthesis of STP3725 for all animal experiments stated were carried out by ST Pharm in a previous study. For in vivo experiments, STP3725 was dissolved in distilled water, followed by the addition of poloxamer 188 (2.16 mg/kg) and labrasol (10 µL/mg STP3725) as solubilizers for the administration dosage of 5 mg/kg. The resulting solution (200 µL) was administered to each mouse by oral gavage.

Statistics

Values are presented as mean±SEM unless otherwise indicated. For in vivo studies, replicates were performed three times, each time containing at least 8–10 individuals. For all data, statistical significance was determined either by Student's t-test between two groups or one-way analysis of variance followed by Turkey's post hoc analysis for multiple-group comparisons. Statistical analysis was performed with GraphPad Prism V.7. Statistical significance was set to $p<0.05$.

Other detailed methods are provided in online supplemental methods.

RESULTS

CAT aggravates hypoxia while reducing immune cell infiltration

In highly thrombotic B16F10.OVA melanoma (Ovalbumin-transfected B16F10 melanoma)-bearing C57BL/6 mice, an induced thrombosis model was established by injecting fluorescently labeled fibrinogen. Fibrinogen-Cy5.5 dosage was varied from low, moderate to high amounts that showed corresponding patterns of fluorescence by IVIS (*In vivo* imaging system) imaging (figure 1A) and this was also quantified (figure 1B) that shows 12.30-fold increase in the 'high' group compared

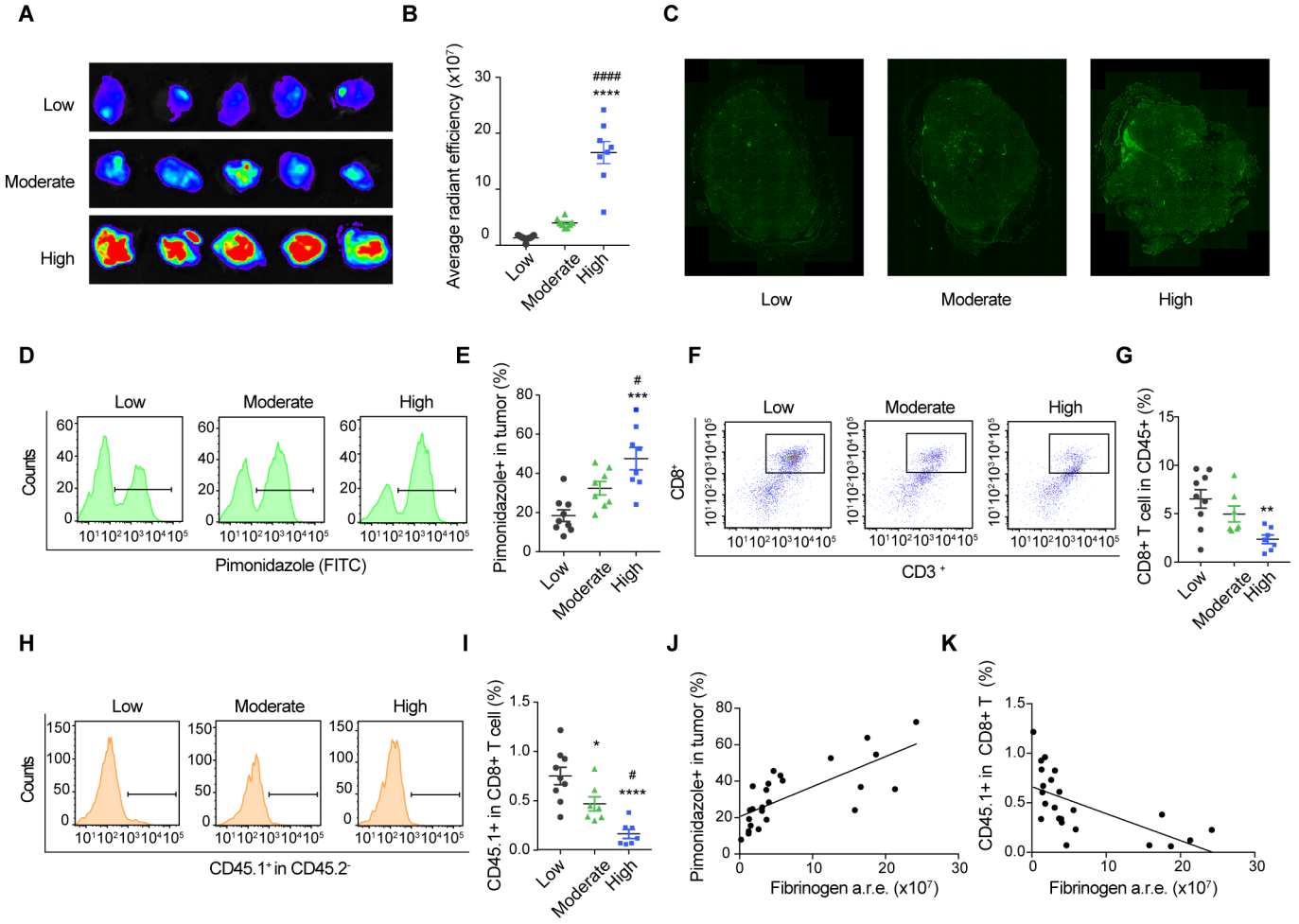

Figure 1 Cancer-associated thrombosis (CAT) aggravates hypoxia while reducing immune cell infiltration. (A, B) Induced thrombosis model of melanoma tumors was observed by varying dosage of fibrinogen-Cy5.5 and tumors imaged ex vivo by IVIS imaging (A) and fluorescence quantified (B). (C–E) Tumor hypoxia was observed by tissue staining for pimonidazole (C), and flow cytometry analysis (D, E). (F, G) Infiltration of CD8 T cells in tumors were analyzed and quantified by flow cytometry. (H, I) Exogenosuly injected CD45.1 congenic lymphocytes were detected (H) and quantified by flow cytometry (I). (J, K) Linear regression analysis showing the relationship between injected fibrinogen and tumor hypoxia (pimonidazole) (J) and the relationship between injected fibrinogen and infiltration of CD45.1 congenic lymphocytes (K). All data represent mean± SEM. *P<0.05, **p<0.01, ***p<0.001, ****p<0.0001 compared with low group and #p<0.05, ####p<0.0001 compared with the moderate group by one-way ANOVA with Turkey's post-test. ANOVA, analysis of variance. FITC, fluorescein isothiocyanate.

with 'low'. Detection of tumor hypoxia by pimonidazole showed an increase in pattern in correlation to fibrinogen-Cy5.5 amount by immunofluorescence staining (figure 1C) and flow cytometry (figure 1D,E) that showed 2.58-fold increase in the 'high' group compared with 'low'.

Subsequently, detection of intratumoral $CD8^+$ T cells showed an inverse correlation to injected fibrinogen-Cy5.5 (figure 1F). Quantified flow cytometry analysis showed that number of T cells decreased by 2.76-fold in the 'high' group compared with 'low' (figure 1G). Similarly, exogenously injected $CD45.1^+$ congenic T lymphocytes were detected harvested tumors of melanoma-bearing wild-type mice to show a decreasing pattern of newly infiltrating lymphocytes (figure 1H) and quantified values showed 4.56-fold decrease in the 'high' group compared with 'low' (figure 1I).

Further, linear regression analysis was performed of the relationship between injected fibrinogen and tumor hypoxia (pimonidazole) (figure 1J) that showed a positive correlation and the relationship between injected fibrinogen and infiltration of $CD45.1^+$ congenic lymphocytes that showed negative correlation (figure 1K).

Overall, these results showed that this induced thrombosis model displays tumor hypoxia exerted by CAT, and that this fibrinogen-mediated limited tumor perfusion shows a corresponding pattern of tumor hypoxia and tumor infiltration of both existing and newly introduced lymphocytes.

Anticoagulation therapy enhances tumor perfusion and reduces hypoxia

In the same melanoma model, various experiments were performed to investigate the effect of anticoagulation

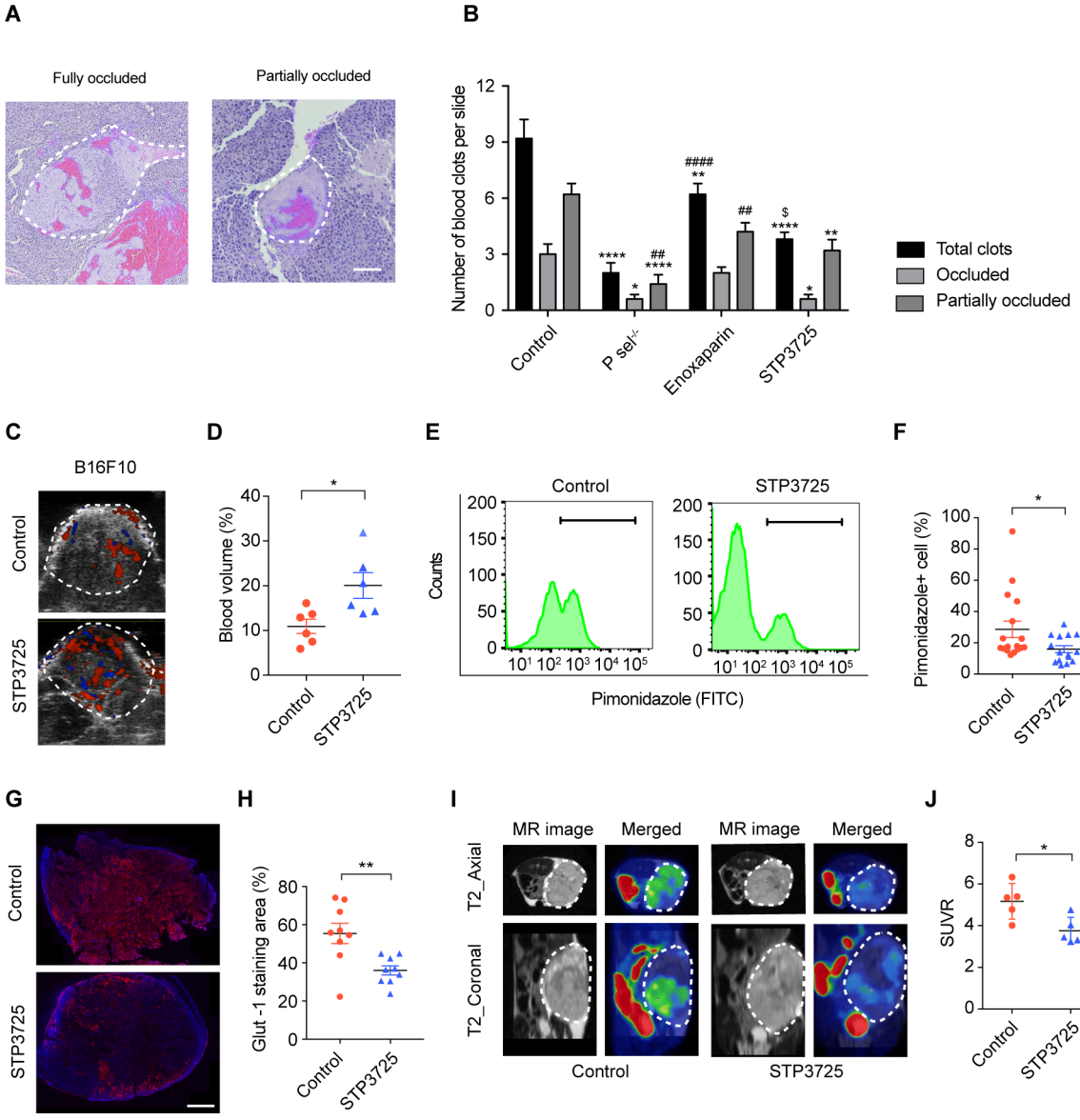

Figure 2 Anticoagulation therapy enhances tumor perfusion and reduces hypoxia. (A, B) B16F10 tumors were sectioned and stained with H&E to show blood clots. Representative slides of fully (left) and partially (right) occluded vessel (A). Scale bar 50 µm. tumors from control, P selectin knock out, enoxaparin-treated and STP3725-treated mice were compared (B). (C) B16F10-bearing mice treated with either the vehicle or STP3725, were imaged with 3D Doppler and (D) in vivo intratumoral blood volumes were measured. (E) Comparison of pimonidazole^{+} (green) hypoxic areas in tumor tissue treated with the vehicle or STP3725, analyzed by flow cytometry and (F) quantified. (G) GLUT-1^{+}(red) hypoxic areas in tumor tissue was shown with confocal microscopy and (H) quantified. Scale bar 2 mm. (I) PET/MR images for detection of[11] FMISO. (J) SUVR (^{18}FMISO intensity in tumor/^{18}FMISO intensity in muscle) values quantified in B16F10 bearing mice treated with the vehicle or STP3725. All data represent mean±SEM. *P<0.05, **p<0.01, ****p<0.0001 compared with the control group, #p<0.05, ##p<0.01, ####p<0.0001 compared with the Psel$^{-/-}$ group, $p<0.05 compared with the enoxaparin group by one-way ANOVA in (B) with Tukey's post-test and Students' t-test in (D, F, H, J). See also online supplemental figures 1 and 2 and online supplemental video 1 and online supplemental video 2. ANOVA, analysis of variance.

therapy on tumor perfusion and hypoxia. P selectin knockout (Psel$^{-/-}$) mice were used for negative control as P selectin is essential for the formation of CAT. Control, P sel$^{-/-}$, enoxaparin- and STP3725-treated mice were evaluated for blood clots (figure 2A) that showed that its incidence was highest in the wild-type mice compared with all other groups (figure 2B). Vessel occlusion caused by CAT was quantified by H&E staining (fully occluded >80%, partially occluded <80%). Enoxaparin-administered mice showed diminished thrombosis compared with control and STP3725 treated group presented even less incidence of clots similar to P sel$^{-/-}$ group (online supplemental figure 1A).

Further, three-dimensional (3D) Doppler analysis was used in this model to visualize and quantify perfusion in the tumor tissue in B16F10 (figure 2C,D). We found that both sectional blood flow and total blood volume in the tumor tissue were increased by

STP3725 administration, also apparent in the 3D tumor images of control (online supplemental video 1 and STP3725-treated mice online supplemental video 2).

Also, similar patterns of perfusion were observed in other tumor types (AsPC-1, CT26) following STP3725 treatment (online supplemental figure 1B–E).

STP3725 enhanced tumor perfusion and subsequently diminished tumor hypoxia, analyzed by flow cytometric analysis that showed hypoxic (pimonidazole$^+$) cells decreased by 44.39±7.64% in STP3725-treated mice compared with control (figure 2E,F). This was also evident by staining the tumor tissue for GLUT-1, overexpressed in hypoxic conditions, that stained significantly less by 35.06±4.32% for tumors in the STP3725-treated mice (figure 2G,H). Subsequently, live imaging of hypoxia in tumor was observed by PET/MR, using[11] FMISO dye, that showed STP3725 diminished the SUVR (Standardized uptake value/region) value by 27.27±5.55% compared with control (figure 2I,J).

Collectively, we conclude that prevention of CAT using anticoagulation therapy can be an effective strategy to enhance tumor perfusion while alleviating hypoxia.

Anticoagulation therapy modulates the tumor immune microenvironment and promotes infiltration of lymphocytes

The alleviation of hypoxia rendered by STP3725 treatment, and its effects on the tumor immune microenvironment was investigated by analyzing hypoxia-related immunosuppressive molecules: HIF-1α; transforming growth factor β; vascular endothelial growth factor A; chemokine ligand 28. STP3725 directly reduced the expression of these proteins (figure 3A–F) compared with control group and this evidently verifies that STP3725 can contribute to the relief of immunosuppression.

Tumor whole slide showed that total level of hypoxia was also lower in the STP3725 group compared with control, but number of infiltrated CD8$^+$ cells were higher (figure 3G). Magnified images showed that CD8$^+$ cells were almost depleted in the pimonidazole$^+$ area in both control and STP3725 groups (figure 3H). This indicates that STP3725 can expand the spatial distribution of lymphocytes within the tumor tissue by alleviating hypoxia.

Further, the effect of STP3725 on the infiltration of new lymphocytes was investigated using a congenic (CD45.1$^+$) mouse model, where harvested lymphocytes were injected into B16F10.OVA tumor-bearing syngeneic wild-type (CD45.2$^+$) mice after immunization of lymphocytes with tumor-specific antigen (figure 3I). Infiltration of new (CD45.1$^+$) lymphocytes in the tumor tissue of receiving mice were higher in STP3725-treated group by 3.96-fold compared with control (figure 3J,K) suggesting that consistent anticoagulation therapy promotes the entry of new lymphocytes into tumor tissue.

Excised tumors were also analyzed for hypoxia following rivaroxaban and STP3725 treatment. Tissue immunofluorescence staining showed a similar pattern of decrease in tumor hypoxia following oral anticoagulation therapy by rivaroxaban and STP3725, and this was quantified by flow cytometry to show the same pattern (online supplemental figure 2A,B). In this tumor model, rivaroxaban or STP3725 treatment did not affect tumor growth compared with control (data not shown). Further, tumor CD8$^+$ T cells were detected by flow cytometry to show increased numbers of T cells for rivaroxaban and STP3725-treated mice (online supplemental figure 2C).

Collectively, the data indicate that STP3725 can enhance the infiltration and spatial distribution of new lymphocytes in the tumor tissue by alleviating hypoxia (online supplemental figure 3).

Anticoagulation therapy potentiates the anticancer efficacy of αPD-1 antibody

After confirming the immune-favorable microenvironment changes induced by STP3725 treatment, this was combined with αPD-1 (anti-programmed cell death protein 1) antibody to show inhibition of tumor growth by 77.26±2.78% in the combination group (figure 4A) in a B16F10.OVA model; STP3725 monotherapy showed marginal effects and antibody monotherapy presented 46.60±7.88% inhibition compared with control without severe toxicity (figure 4B–D). Effective tumor growth inhibition was also confirmed in a mouse colorectal CT26.CL25 model (figure 4E–H).

STP3725 treatment also significantly improved both the distribution and the accumulation of αPD-1 antibody-Cy5.5 in the tumor tissue by 1.92-fold compared with control (online supplemental figure 4) indicating that STP3725 administration promotes αPD-1 antibody delivery and distribution in the tumor tissue possibly by promoting tumor perfusion. Furthermore, higher CD8$^+$ TIL numbers and diminished hypoxia was observed in the combination therapy compared with αPD-1 group (online supplemental figure 5). These results correlated with the enhanced anti-tumor efficacy and indicate synergistic benefits of the combination therapy.

A highly immune-depleted mouse pancreatic Pan02 model was also investigated, and the results showed similar patterns of promotion of αPD-1 antibody efficacy in inhibiting tumor growth (online supplemental figure 6).

Combination of anticoagulant and αPD-1 antibody promotes the infiltration of effector lymphocytes

Analysis of immune cell changes after STP3725 administration in a B16F10.OVA model showed increases in the population of TIL (CD45$^+$), cytotoxic T cells (CD3$^+$CD8$^+$) and helper T cells (CD3$^+$CD4$^+$) compared with control, and the combination group showed highest populations (figure 5A–C). There were no significant differences in the regulatory T cells (CD4$^+$foxp3$^+$) numbers, however, the increase in ratio of cytotoxic to regulatory T cells was meaningful only in the combination group (figure 5D,E). Interestingly, STP3725 treatment reduced the myeloid-derived suppressor cell (MDSC) (CD11b$^+$Gr-1$^+$)

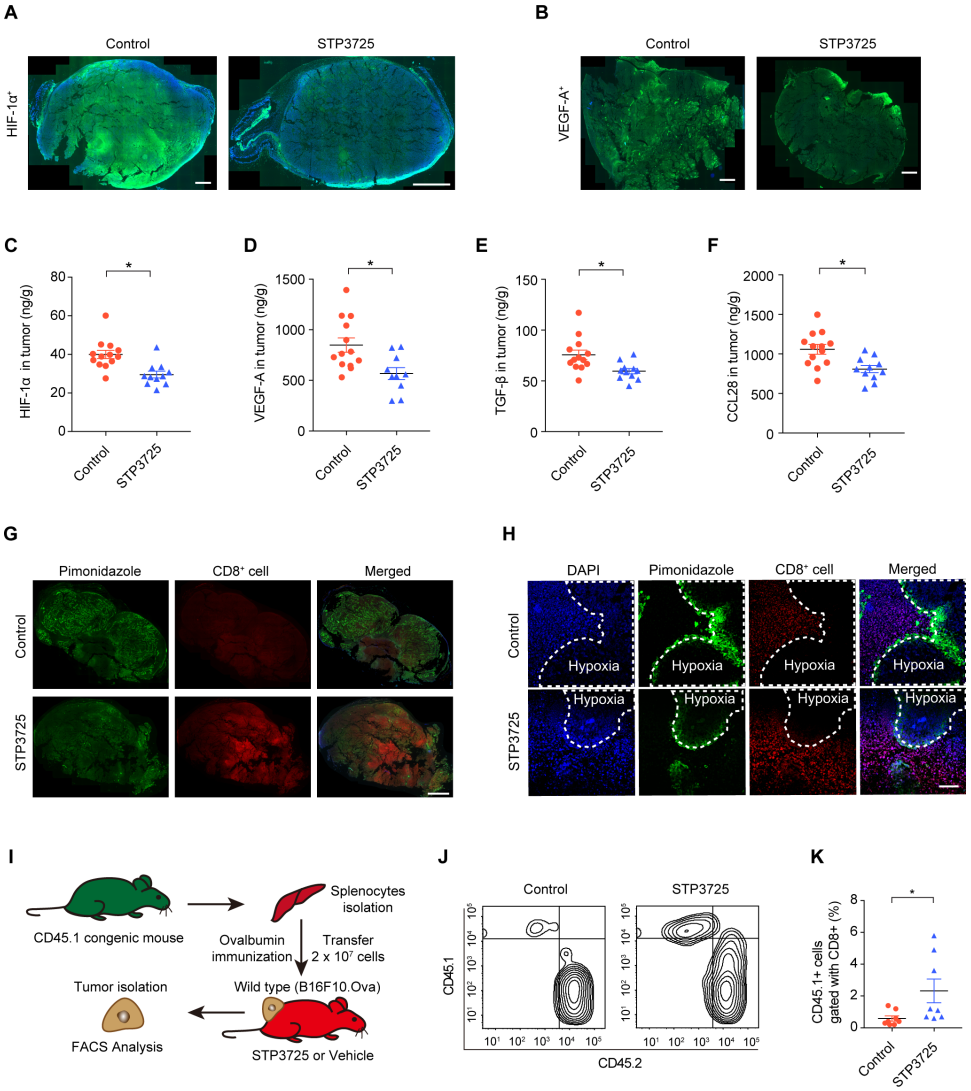

Figure 3 Anticoagulation therapy modulates the tumor immune microenvironment and promotes infiltration of lymphocytes. (A, B) Staining of HIF1α$^+$ (green) (A) and VEGF-A$^+$ (green) (B) in B16F10 tumor tissue slide from vehicle or STP3725-treated mice. Scale bar 2 mm. (C–F) hypoxia-related cytokines HIF1α (C) VEGF-A (D), TGF-β (E) and CCL28 (F) were quantified in whole tumor lysate using ELISA. (G) Costaining of pimonidazole$^+$(green) hypoxic region and CD8$^+$ (red) cells in whole tumor slide (H) and magnified images from vehicle (above) or STP3725-treated (below) mice to identify the spatial distribution of CD8$^+$ cells in hypoxic region. Scale bar 3 mm in (G), 100 µm in (H). (I) Diagram depicting lymphocyte transfer model using congenic (CD45.1$^+$) and wild-type (CD45.2$^+$) C57BL/6 mice with B16F10.OVA tumor. (J) Representative flow cytometric plots showing wild-type CD45.2$^+$ and exogenously injected congenic CD45.1$^+$ lymphocytes, (K) quantified. All data represent mean±SEM. *P<0.05 compared with the control group, by Student's t-test. See also online supplemental figure 3. CCL28, chemokine ligand 28; HIF1α, hypoxia-inducing factor-1α; VEGF, vascular endothelial growth factor; TGF-β, transforming growth factor β; FACS, fluorescence-activated cell sorting analysis.

populations compared with control, and the pattern was the same for combination group compared with αPD-1 monotherapy (figure 5F). Here, αPD-1 monotherapy exerted no changes and it can be deduced that STP3725 was solely responsible for the reduction of MDSCs. Similarly, only in the combination group did the ratio of cytotoxic T cells to MDSCs show significant increase compared with both the control and αPD-1 monotherapy groups (figure 5G).

Evaluation of cytotoxic T cell function showed that PD-1$^+$ mean fluorescence intensity (MFI) were lowered after STP3725 treatment regardless of αPD-1 treatment (figure 5H); also, the population of Ki67$^+$ cells were highest in the combination group (figure 5I). T cell functions in tumor were further investigated by showing that STP3725 and the combination groups substantially enhanced interferon gamma (IFNγ) secretion of OVA-stimulated B16F10.OVA tumor-derived lymphocytes (figure 5J). Similarly, numbers of IFNγ, tumor necrosis factor alpha (TNFα)-releasing CD8$^+$ T cell and 'polyfunctional T cell' (IFNγ$^+$TNFα$^+$) showed the same patterns (figure 5K,L). Based on the data that show reduction of PD-1-expressing T cells and increase in proliferating

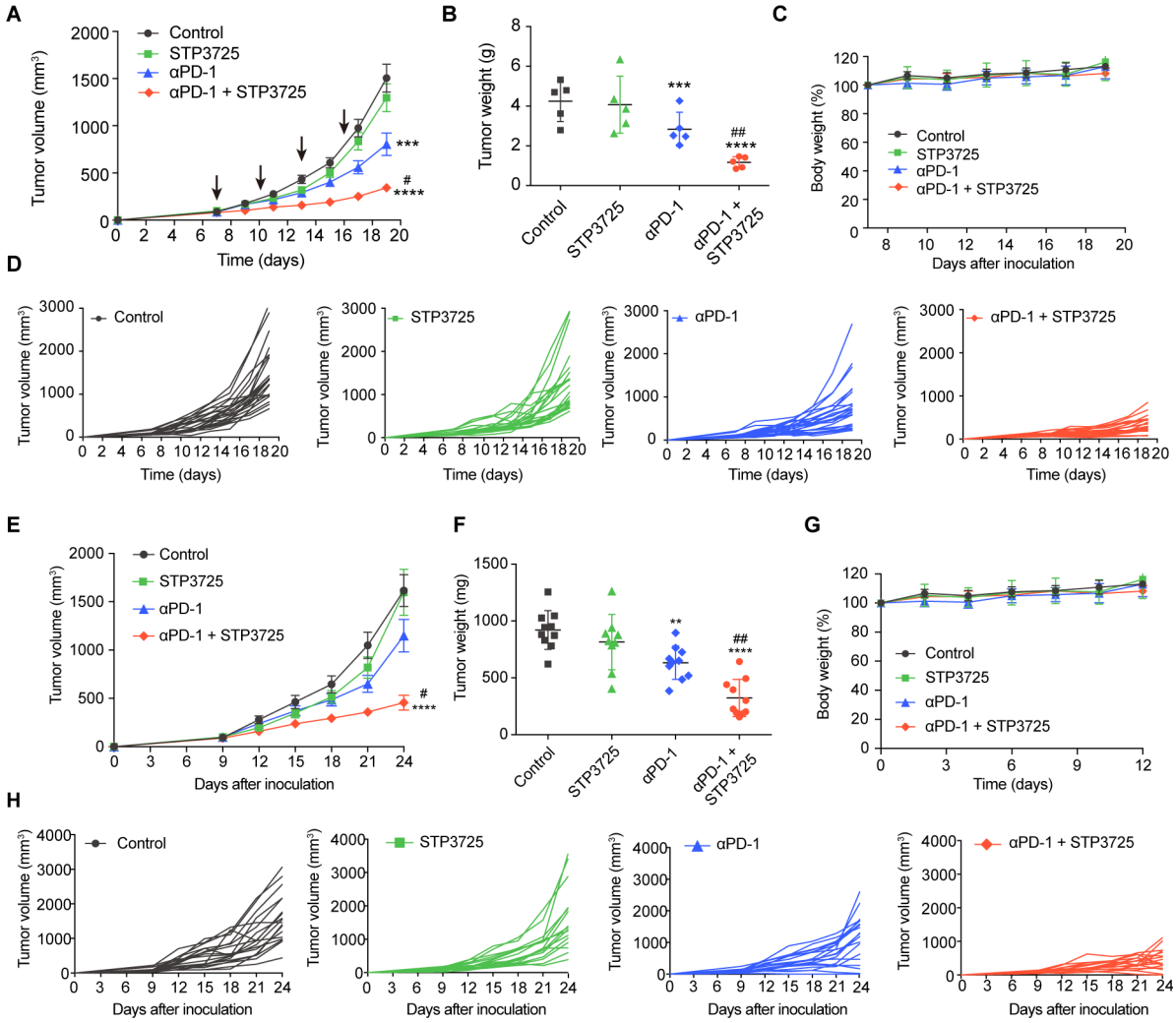

Figure 4 Anticoagulant therapy potentiates the anticancer efficacy of αPD-1 antibody. (A–D) (A) Comparison of B16F10.OVA tumor growth inhibition in control, STP3725, αPD-1 and combination groups. (B) Tumors harvested on day 19 were weighed. (C) Body weight changes and (D) individual tumor growth. (E–H) similarly, tumor growth inhibition in the same groups were measured using CT26.CL25 tumor model. (F) Tumors harvested on day 24 were weighed. (G) Body weight changes and (H) individual tumor growth. All data represent mean±SEM. **p<0.01, ***p<0.001, ****p<0.0001 compared with the control group, #p<0.05, ##p<0.01 compared with the STP3725 group by one-way ANOVA with Tukey's post-test. See also online supplemental figures 4 and 5. ANOVA, analysis of variance.

and cytokine-secreting T cells in tumor, we contend that STP3725 also improved the function of cytotoxic T cells. All data was analyzed in comparison to the corresponding IgG antibody data (online supplemental figure 7).

Additionally, in a CT26.CL25 model, STP3725 also exerted increase in TILs, cytotoxic T cells and helper T cells, while reducing MDSCs and PD-1$^-$ CD8$^+$ T cells in tumor (online supplemental figure 5); these results collectively confirm again, the alteration of the tumor immune microenvironment by STP3725.

Overall, STP3725 significantly enhanced the efficacy of αPD-1 antibody by reducing MDSC population while enhancing both the numbers and function of T cells.

Combination therapy promotes tumor-specific memory responses

Additionally, tumor (OVA)-specific immune responses were assessed by measuring IFNγ levels after stimulating tumor-derived lymphocytes and splenocytes with tumor specific antigen from B16F10.OVA-bearing mice (figure 6A). The results showed highest IFNγ levels in the combination group analyzed by ELIspot as depicted in the representative images and quantitative analysis of the spotting in tumor derived lymphocytes (figure 6B,C). Splenocytes also presented similar results, in that the combination group showed highest IFNγ levels in ELIspot as well as and ELISA (figure 6D,E). It is important to note that STP3725 monotherapy showed negligible results on IFNγ levels, which implies that anticoagulant alone is not enough to exert a strong local or systemic immune memory response. Collectively, these data suggest that combination of anticoagulant and immunotherapy can strongly elicit tumor specific memory responses both for local and systemic manner.

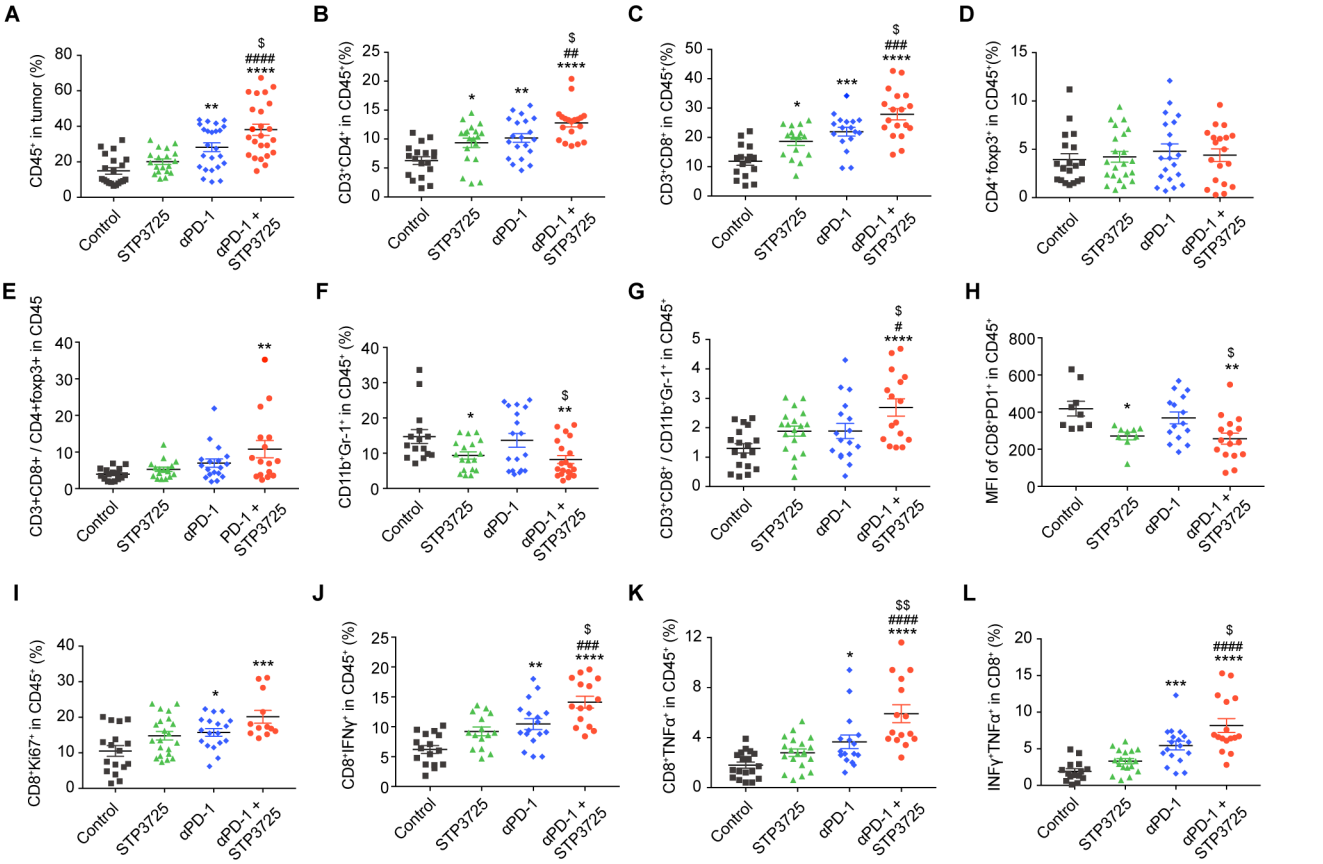

Figure 5 Combination of anticoagulant and αPD-1 antibody promotes the infiltration of effector lymphocytes. (A) Flow cytometry analysis of CD45$^+$ cell fraction in whole B16F10.OVA tumor and CD45$^+$-gated cells for (B) CD3$^+$CD4$^+$ T cells, (C) CD3$^+$CD8$^+$ T cells, (D) regulatory T cells, (E) ratio of CD8$^+$ cells/regulatory T cells, (F) MDSCs, (G) ratio of CD8$^+$ cells/MDSCs, (H) PD-1$^-$CD8$^+$ T cells, and (I) proliferating CD8$^+$ T cells in each group. Cytokine-secreting CD8$^+$ cells such as (J) IFNγ-secreting CD8$^+$ T cells, (K) TNFα-secreting CD8$^+$ T cells, (L) IFNγ$^+$TNFα$^+$CD8$^+$ T cells (poly functional T cell) were also analyzed. All data represent mean±SEM. *P<0.05, **p<0.01, ***p<0.001, ****p<0.0001 compared with the control group, #p<0.05, ##p<0.01, ###p<0.001, ####p<0.0001 compared with the STP3725 group, $p<0.05, $$p<0.01 compared with the αPD-1 group, by one-way ANOVA with Tukey's post-test. See also online supplemental figures 6 and 7. ANOVA, analysis of variance; IFNγ, interferon-γ; MDSC, myeloid-derived suppressor cell; TNFα, tumor necrosis factor-α.

Combination therapy attenuates tumor development in a *K-ras* mutant mouse model

The efficacy of STP3725 combination with αPD-1 antibody was previously verified in various syngeneic/orthotopic tumor models and the same regimen was also applied in the highly thrombotic *K-Ras* mutant spontaneous lung cancer mouse model. After treatment of drugs, mice were sacrificed and the lungs were harvested and imaged (figure 7A,B). We found that while STP3725 monotherapy mediated negligible changes compared with control, the combination with αPD-1 antibody substantially reduced nodule formation, lung weight and tumor area fractions in the H&E slides (figure 7C–F). The MSB staining showed that STP3725 significantly attenuated clot incidence in both intratumoral and non-tumoral areas of the lung tissue (figure 7G,H). In conclusion, the treatment of STP3725 considerably diminished the thrombotic incidences and the combination of STP3725 and αPD-1 antibody substantially attenuated spontaneous lung cancer development in this model. Based on these results, we postulate that the potentiation of anticancer effects of αPD-1 antibody in this *K-Ras* mutant model is also attributable to the improved tumor immune-microenvironment resulted from reduced hypoxia and incidence of CAT.

DISCUSSION

In this study, we verified systematically that CAT serves as a major perfusion barrier, which limits oxygen supply in tumor and prevention of CAT using oral anticoagulation therapy effectively reduces hypoxia. Furthermore, the enhanced perfusion alleviated tumor hypoxia, resulting in the alteration of the TME into an 'immune-supportive' state that reduced the expression of immunosuppressive cytokines and MDSC populations, which in turn, facilitated the entry of new lymphocytes.

STP3725 treatment also increased the ratio of PD-1 negative to positive CD8$^+$ T cells in tumors. Hypoxic and glucose-limited TME is associated with the expression of checkpoint molecules, such as PD-1, LAG-3 and CTLA-4 on T cells in the tumor, the markers of exhaustion.[33 34]

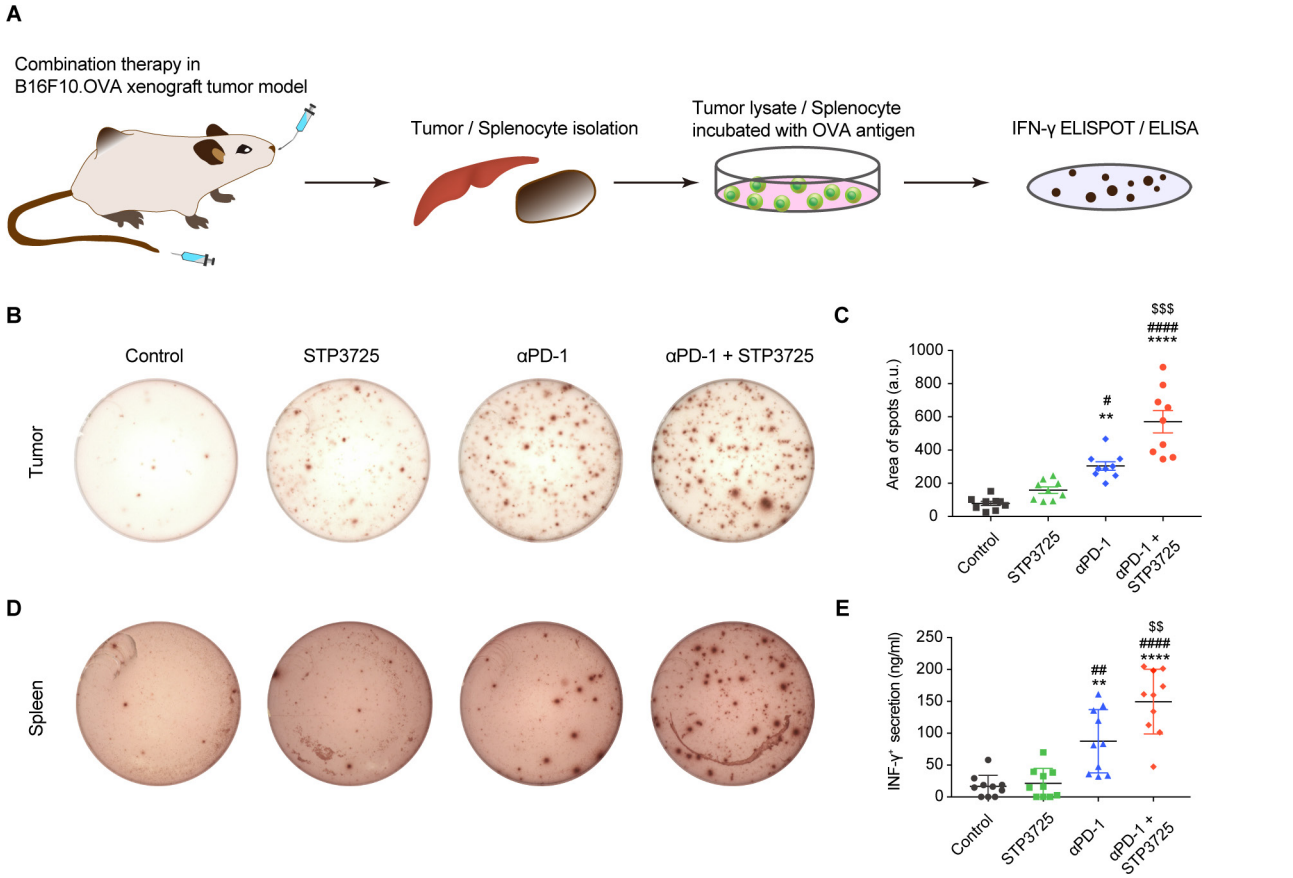

Figure 6 Combination therapy promotes tumor-specific memory responses. (A) Diagram depicting the tumor antigen specific T cell response ex vivo model using IFNγ ELISPOT and ELISA. (B) IFNγ ELISpot images were acquired after stimulating splenocytes with OVA from the tumor tissues in each group and (C) area of dot was quantified in each group. (D) Similarly, IFNγ ELISpot images were acquired after stimulating splenocytes with OVA from the splenocytes in each group and (E) the amount of IFNγ in splenocytes cultured media after OVA stimulation was measured using ELISA. IFNγ, interferon γ. All data represent mean±SEM. **p<0.01, ****p<0.0001 compared with the control group, #p<0.05, ##p<0.01, ####p<0.0001 compared with the STP3725 group, $$p<0.01, $$$p<0.001 compared with the αPD-1 group, by one-way ANOVA with Tukey's post-test.

Thus, we contend that the alleviation of hypoxia and the increased number of newly infiltrated T cells following STP3725 treatment contribute to this increase in the number of PD-1 negative $CD8^+$ T cells.

In addition, STP3725 is responsible for the reduction of MDSC regardless of the αPD-1 antibody co-administration. Based on several studies which revealed that hypoxia-dependent HIF-1α is highly associated to MDSC levels in the TME,[35 36] we can presume that the observed decrease in the cytokine levels after STP3725 treatment is responsible for the reduction in MDSC population. As circulating MDSC level inversely correlate with the overall survival and clinical outcomes of immunotherapies,[37 38] MDSC reduction after STP3725 treatment could be an additional benefit that improves the efficacy of immunotherapeutic agents.

Heparin is known for exerting various immunological and biological effects that may affect the tumor and its microenvironment.[39–41] In order to demonstrate that tumor hypoxia was diminished by the anticoagulation effect, we compared STP3725 to an existing DOAC, rivaroxaban in the same tumor model. Both anticoagulant drugs resulted in a decrease in tumor hypoxia and increase in $CD8^+$ T cells, but STP3725 was similar or slightly more effective compared with rivaroxaban. From these results, we can postulate that heparin mediates additional effects to anticoagulation that contribute to its merit over rivaroxaban, but further studies are required to clearly demonstrate this.

We next selected the *K-Ras* mutation mouse model, in which all mice developed lung cancer spontaneously; this model was chosen as the mouse phenotype has high incidence of CAT, deriving from the mutation[42] and this model can simulate the features of the *Ras* mutant cancers relevant to clinics.[43] We were able to validate the effects of STP3725 on reducing the formation of CAT and on enhancing the efficacy of αPD-1 antibody in a spontaneous cancer model. We expect that this strategy, proven effective in this model, will be applicable to highly thrombotic solid tumors.

CAT formation is an inevitable element persistent during tumor development and methods to treat CAT in patients with cancer is actively pursued in the clinic[44]; thus, it is appealing to use its role of a perfusion limiting barrier as a target for a combination regimen consisting of anticoagulants and immunotherapies. As anticoagulation

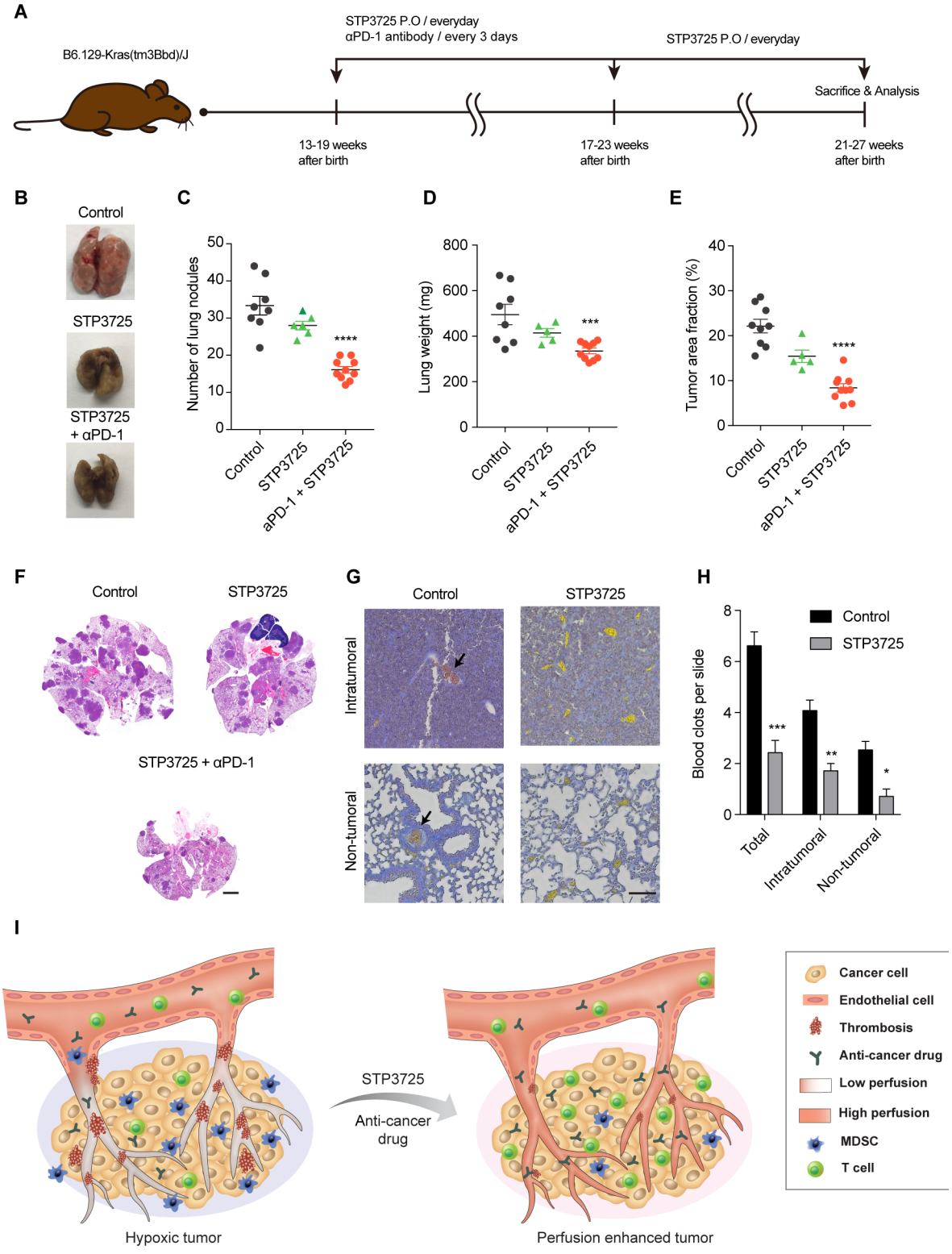

Figure 7 Combination therapy attenuates tumor development in a in *K-ras* mutant mouse model. (A) Schematic figure depicting the dosing schedule in *K-ras* mutant model. (B) Representative images of lung tissues harvested from vehicle, STP3725, and STP3725+αPD-1 antibody-treated mice. (C) Quantification of lung nodules, (D) lung weight, (E) and total tumor area fraction of lung tissues. (F) Representative whole tissue image was shown. Scale bar 2 mm. (G) Fibrin clots in lung tissue slides were distinguished both in tumor and non-tumoral areas using MSB (Lendrum) staining method (H) and quantified. (I) Schematic diagram depicting changes in the tumor immune microenvironment following anticoagulant treatment. STP3725 treatment enhances the blood flow into the tumor tissue while alleviates tumor hypoxia, which leads to changes in the composition and population of immune cells (MDSCs and T cells). Scale bar 100 µm. All data represent mean±SEM. *P<0.05, **p<0.01, ***p<0.001, ****p<0.0001 compared with control group and one-way ANOVA in (C–E) and two-way ANOVA in (H) with Turkey's post-test. ANOVA, analysis of variance; MDSCs, myeloid-derived suppressor cell.

therapy can be used to enhance the efficacy of immunotherapy, STP3725 may also be combined with other hypoxia-relieving strategies for a synergistic effect in enhancing anti-tumor immunity.[13]

As long-term treatment and prevention of VTE still remain a problem for cancer patients,[29 45] a new combinatorial protocol consisting of a new oral anticoagulant and immunotherapies could generate synergistic therapeutic benefits for patients with cancer. Although the use of anticoagulants in cancer patients require caution because of the heightened risk of hemorrhage,[46 47] a systematic scoring system of evaluating CAT including the 'Khorana score' can help to predict the risk of VTE.[48 49] We expect that the benefits of our combinatorial strategy can far outweigh the disadvantages of using anticoagulants alone.

In conclusion, STP3725, the orally active enoxaparin, can enhance tumor perfusion and alleviate hypoxia by preventing CAT, to help enhance the efficacy of immunotherapies by fostering an immune-supportive microenvironment (figure 7I). This strategy has strong potential for expanding the combinatorial criteria of anticoagulation therapy to include other types immunotherapies and appears highly appropriate for clinical translation.

Author affiliations
[1]Research Institute of Pharmaceutical Sciences, College of Pharmacy, Chonnam National University, Gwangju, South Korea
[2]Research Institute of Pharmaceutical Sciences, College of Pharmacy, Seoul National University, Gwanak-gu, South Korea
[3]La Jolla Institute for Immunology, La Jolla, California, USA
[4]Center for Nanomedicine, Wilmer Eye Institute, Johns Hopkins University, Baltimore, Maryland, USA
[5]Department of Pharmaceutical Sciences, School of Pharmacy, University of Texas at El Paso, El Paso, Texas, USA
[6]Department of Molecular Medicine and Biopharmaceutical Sciences, Graduate School of Convergence Science and Technology, Seoul National University, Seoul, South Korea
[7]Laboratory Animal Center, Daegu Gyeongbuk Medical Innovation Foundation, Daegu, South Korea
[8]ST Pharm Research & Development Center, Siheung-si, South Korea
[9]Department of Biomedicine, Health & Life Convergence Sciences, BK21 Four, Biomedical and Healthcare Research Institute, Mokpo National University, Jeonnam, South Korea
[10]Center for Theragnosis, Biomedical Research Institute, Korea Institute of Science and Technology, Seongbuk-gu, South Korea
[11]College of Medicine, University of Ulsan, Ulsan, South Korea
[12]Department of Otolaryngology, Asan Medical Center, Seoul, South Korea

Twitter Seong Jin Park @Seong-jin Park

Acknowledgements The authors gratefully acknowledge the support of this work by ST Pharm (Republic of Korea). We would like to extend our appreciation to Dr. Hyun-Bae Ji (Ambrx, CA USA) for his comments. We would also like to thank Dr. Woo-Chan Son (Department of Pathology, Asan Medical Centre, Republic of Korea) for the examination of the CAT histological samples. The authors thank H.J. Noh of the National Center for Inter-university Research Facilities (NCIRF) (Republic of Korea) for assistance with the flow cytometry analysis. Lastly, we greatly appreciate Gi-Hoon Nam (Korea Institute of Science& Running title: Anticoagulation therapy potentiates the efficacy of immunotherapy by relieving tumor hypoxia Technology) and Eun Ah Bae (Sanford Burnham Prebys Medical Discovery Institute, CA, USA) for their guidance in the experimental procedures.

Collaborators The authors gratefully acknowledge the support of this work by ST Pharm (Republic of Korea). We would like to extend our appreciation to Dr. Hyun-Bae Ji (Ambrx, CA USA) for his comments. We would also like to thank Dr. Woo-Chan Son (Department of Pathology, Asan Medical Centre, Republic of Korea) for the examination of the CAT histological samples. The authors thank H.J. Noh of the National Center for Inter-university Research Facilities (NCIRF) (Republic of Korea) for assistance with the flow cytometry analysis. Lastly, we greatly appreciate Gi-Hoon Nam (Korea Institute of Science& Technology) and Eun Ah Bae (Sanford Burnham Prebys Medical Discovery Institute, CA USA) for their guidance in the experimental procedures.

Contributors JUC and NKL contributed equally. JUC designed all experiments; JUC and NKL conducted experiments, analyzed data, and wrote the manuscript. HS, SWC, TAA-H, SA, U-IK, JWP, C-YK, I-SK, SYK participated in the analysis, interpretation and discussion of experiments and preparation of the manuscript. SKK, SJP, SK, NM assisted in the experimental procedures. KK and YB supervised the overall project. Correspondence and requests for materials should be addressed to YB.

Funding This work was supported by the National Research Foundation (NRF) of Korea funded by the Ministry of Science (No. 2020R1A2C2015026 and 2016M3A9B5941836).

Competing interests No, there are no competing interests.

Patient consent for publication Not required.

Ethics approval All animal care and experimental procedures were performed in accordance with guidelines of the Institute of Laboratory Animal Resources Seoul National University (SNU) approval number SNU-170502-3-2.

Provenance and peer review Not commissioned; externally peer reviewed.

Data availability statement Data are available upon reasonable request. Youngro Byun http://orcid.org/0000-0002-3863-2236

ORCID iDs
In-San Kim http://orcid.org/0000-0003-1714-4521
Youngro Byun http://orcid.org/0000-0002-3863-2236

REFERENCES

1 Park J-S, Kim I-K, Han S, *et al*. Normalization of tumor vessels by Tie2 activation and Ang2 inhibition enhances drug delivery and produces a favorable tumor microenvironment. *Cancer Cell* 2016;30:953–67.
2 Jain RK. Antiangiogenesis strategies revisited: from starving tumors to alleviating hypoxia. *Cancer Cell* 2014;26:605–22.
3 Stylianopoulos T, Jain RK. Combining two strategies to improve perfusion and drug delivery in solid tumors. *Proc Natl Acad Sci U S A* 2013;110:18632–7.
4 Chauhan VP, Stylianopoulos T, Martin JD, *et al*. Normalization of tumour blood vessels improves the delivery of nanomedicines in a size-dependent manner. *Nat Nanotechnol* 2012;7:383–8.
5 Mukai M, Oka T. Mechanism and management of cancer-associated thrombosis. *J Cardiol* 2018;72:89–93.
6 Caldwell CC, Kojima H, Lukashev D, *et al*. Differential effects of physiologically relevant hypoxic conditions on T lymphocyte development and effector functions. *J Immunol* 2001;167:6140–9.
7 Lukashev D, Caldwell C, Ohta A, *et al*. Differential regulation of two alternatively spliced isoforms of hypoxia-inducible factor-1 alpha in activated T lymphocytes. *J Biol Chem* 2001;276:48754–63.
8 Cramer T, Yamanishi Y, Clausen BE, *et al*. Hif-1Alpha is essential for myeloid cell-mediated inflammation. *Cell* 2003;112:645–57.
9 Palazon A, Tyrakis PA, Macias D, *et al*. An HIF-1α/VEGF-A axis in cytotoxic T cells regulates tumor progression. *Cancer Cell* 2017;32:669–83.

10 Doedens AL, Phan AT, Stradner MH, *et al*. Hypoxia-inducible factors enhance the effector responses of CD8(+) T cells to persistent antigen. *Nat Immunol* 2013;14:1173–82.
11 Sitkovsky MV, Hatfield S, Abbott R, *et al*. Hostile, hypoxia-A2-adenosinergic tumor biology as the next barrier to overcome for tumor immunologists. *Cancer Immunol Res* 2014;2:598–605.
12 Kojima H, Gu H, Nomura S, *et al*. Abnormal B lymphocyte development and autoimmunity in hypoxia-inducible factor 1alpha -deficient chimeric mice. *Proc Natl Acad Sci U S A* 2002;99:2170–4.
13 Hatfield SM, Sitkovsky MV. Antihypoxic oxygenation agents with respiratory hyperoxia to improve cancer immunotherapy. *J Clin Invest* 2020;130:5629–37.
14 Semenza GL. Pharmacologic targeting of hypoxia-inducible factors. *Annu Rev Pharmacol Toxicol* 2019;59:379–403.
15 Hatfield SM, Sitkovsky M. A2A adenosine receptor antagonists to weaken the hypoxia-HIF-1α driven immunosuppression and improve immunotherapies of cancer. *Curr Opin Pharmacol* 2016;29:90–6.
16 Hatfield SM, Kjaergaard J, Lukashev D, *et al*. Immunological mechanisms of the antitumor effects of supplemental oxygenation. *Sci Transl Med* 2015;7:277ra30.
17 Hatfield SM, Kjaergaard J, Lukashev D, *et al*. Systemic oxygenation weakens the hypoxia and hypoxia inducible factor 1α-dependent and extracellular adenosine-mediated tumor protection. *J Mol Med* 2014;92:1283–92.
18 Hatfield SM, Sitkovsky M. Oxygenation to improve cancer vaccines, adoptive cell transfer and blockade of immunological negative regulators. *Oncoimmunology* 2015;4:e1052934.
19 Steingold JM, Hatfield SM. Targeting Hypoxia-A2A adenosinergic immunosuppression of antitumor T cells during cancer immunotherapy. *Front Immunol* 2020;11:570041.
20 Kjaergaard J, Hatfield S, Jones G, *et al*. A_{2A} adenosine receptor gene deletion or synthetic A_{2A} antagonist liberate tumor-reactive $CD8^+$ T cells from tumor-induced immunosuppression. *J Immunol* 2018;201:782–91.
21 Sorrentino C, Hossain F, Rodriguez PC, *et al*. Adenosine A2A receptor stimulation inhibits TCR-induced Notch1 activation in CD8+T-Cells. *Front Immunol* 2019;10:162.
22 Khorana AA, Francis CW, Culakova E, *et al*. Frequency, risk factors, and trends for venous thromboembolism among hospitalized cancer patients. *Cancer* 2007;110:2339–46.
23 Timp JF, Braekkan SK, Versteeg HH, *et al*. Epidemiology of cancer-associated venous thrombosis. *Blood* 2013;122:1712–23.
24 Chew HK, Wun T, Harvey D, *et al*. Incidence of venous thromboembolism and its effect on survival among patients with common cancers. *Arch Intern Med* 2006;166:458–64.
25 Ay C, Pabinger I, Cohen AT. Cancer-Associated venous thromboembolism: burden, mechanisms, and management. *Thromb Haemost* 2017;117:219–30.
26 Brat DJ, Van Meir EG. Vaso-occlusive and prothrombotic mechanisms associated with tumor hypoxia, necrosis, and accelerated growth in glioblastoma. *Lab Invest* 2004;84:397–405.
27 Kirtane AR, Sadhukha T, Kim H, *et al*. Fibrinolytic enzyme Cotherapy improves tumor perfusion and therapeutic efficacy of anticancer nanomedicine. *Cancer Res* 2017;77:1465–75.
28 Sharma BK, Flick MJ, Palumbo JS. Cancer-Associated thrombosis: a two-way street. *Semin Thromb Hemost* 2019;45:559–68.
29 Khorana AA, Francis CW. Risk prediction of cancer-associated thrombosis: appraising the first decade and developing the future. *Thromb Res* 2018;164 Suppl 1:S70–6.
30 Wang J, Zhu C. Anticoagulation in combination with antiangiogenesis and chemotherapy for cancer patients: evidence and hypothesis. *Onco Targets Ther* 2016;9:4737–46.
31 Falanga A, Vignoli A, Diani E, *et al*. Comparative assessment of low-molecular-weight heparins in cancer from the perspective of patient outcomes and survival. *Patient Relat Outcome Meas* 2011;2:175–88.
32 Park J, Jeon OC, Yun J, *et al*. End-Site-Specific conjugation of enoxaparin and Tetradeoxycholic acid using nonenzymatic glycosylation for oral delivery. *J Med Chem* 2016;59:10520–9.
33 Lequeux A, Noman MZ, Xiao M, *et al*. Impact of hypoxic tumor microenvironment and tumor cell plasticity on the expression of immune checkpoints. *Cancer Lett* 2019;458:13–20.
34 Zhang Y, Ertl HCJ, Starved EHC. Starved and asphyxiated: how can CD8(+) T cells within a tumor microenvironment prevent tumor progression. *Front Immunol* 2016;7:32.
35 Noman MZ, Desantis G, Janji B, *et al*. Pd-L1 is a novel direct target of HIF-1α, and its blockade under hypoxia enhanced MDSC-mediated T cell activation. *J Exp Med* 2014;211:781–90.
36 Corzo CA, Condamine T, Lu L, *et al*. HIF-1α regulates function and differentiation of myeloid-derived suppressor cells in the tumor microenvironment. *J Exp Med* 2010;207:2439–53.
37 Lang S, Bruderek K, Kaspar C, *et al*. Clinical relevance and suppressive capacity of human myeloid-derived suppressor cell subsets. *Clin Cancer Res* 2018;24:4834–44.
38 Draghiciu O, Lubbers J, Nijman HW, *et al*. Myeloid derived suppressor cells-An overview of combat strategies to increase immunotherapy efficacy. *Oncoimmunology* 2015;4:e954829.
39 Najidh S, Versteeg HH, Buijs JT. A systematic review on the effects of direct oral anticoagulants on cancer growth and metastasis in animal models. *Thromb Res* 2020;187:18–27.
40 Borsig L. Antimetastatic activities of heparins and modified heparins. experimental evidence. *Thromb Res* 2010;125 Suppl 2:S66–71.
41 Niers TMH, Klerk CPW, DiNisio M, *et al*. Mechanisms of heparin induced anti-cancer activity in experimental cancer models. *Crit Rev Oncol Hematol* 2007;61:195–207.
42 Corrales-Rodriguez L, Soulières D, Weng X, *et al*. Mutations in NSCLC and their link with lung cancer-associated thrombosis: a case-control study. *Thromb Res* 2014;133:48–51.
43 Chung W-J, Daemen A, Cheng JH, *et al*. *Kras* mutant genetically engineered mouse models of human cancers are genomically heterogeneous. *Proc Natl Acad Sci U S A* 2017;114:E10947–55.
44 Fernandes CJ, Calderaro D, Piloto B, *et al*. Extended anticoagulation after venous thromboembolism: should it be done? *Ther Adv Respir Dis* 2019;13:1753466619878556.
45 Mahajan A, Wun T. Biomarkers of cancer-associated thromboembolism. *Cancer Treat Res* 2019;179:69–85.
46 Mulder FI, Di Nisio M, Ay C, *et al*. Clinical implications of incidental venous thromboembolism in cancer patients. *Eur Respir J* 2020;55:1901697.
47 Sanfilippo KM, Wang T-F. Prevention and treatment of cancer-associated venous thromboembolism: a review. *Curr Treat Options Cardiovasc Med* 2019;21:70.
48 Khorana AA, Kuderer NM, Culakova E, *et al*. Development and validation of a predictive model for chemotherapy-associated thrombosis. *Blood* 2008;111:4902–7.
49 Fuentes HE, Tafur AJ, Caprini JA, *et al*. Prediction of early mortality in patients with cancer-associated thrombosis in the RIETE database. *Int Angiol* 2019;38:173–84.